Regulation of the transient receptor potential channel TRPM3 by phosphoinositides

Balázs I. Tóth,[1] Maik Konrad,[3] Debapriya Ghosh,[1] Florian Mohr,[3] Christian R. Halaszovich,[3] Michael G. Leitner,[3] Joris Vriens,[1,2] Johannes Oberwinkler,[3] and Thomas Voets[1]

[1]Laboratory of Ion Channel Research and TRP Research Platform Leuven (TRPLe) and [2]Laboratory of Obstetrics and Experimental Gynaecology, KU Leuven, 3000 Leuven, Belgium
[3]Institut für Physiologie und Pathophysiologie, Philipps-Universität Marburg, 35037 Marburg, Germany

The transient receptor potential (TRP) channel TRPM3 is a calcium-permeable cation channel activated by heat and by the neurosteroid pregnenolone sulfate (PregS). TRPM3 is highly expressed in sensory neurons, where it plays a key role in heat sensing and inflammatory hyperalgesia, and in pancreatic β cells, where its activation enhances glucose-induced insulin release. However, despite its functional importance, little is known about the cellular mechanisms that regulate TRPM3 activity. Here, we provide evidence for a dynamic regulation of TRPM3 by membrane phosphatidylinositol phosphates (PIPs). Phosphatidylinositol 4,5-bisphosphate (PI[4,5]P_2) and ATP applied to the intracellular side of excised membrane patches promote recovery of TRPM3 from desensitization. The stimulatory effect of cytosolic ATP on TRPM3 reflects activation of phosphatidylinositol kinases (PI-Ks), leading to resynthesis of PIPs in the plasma membrane. Various PIPs directly enhance TRPM3 activity in cell-free inside-out patches, with a potency order $PI(3,4,5)P_3 > PI(3,5)P_2 > PI(4,5)P_2 \approx PI(3,4)P_2 \gg PI(4)P$. Conversely, TRPM3 activity is rapidly and reversibly inhibited by activation of phosphatases that remove the 5-phosphate from PIPs. Finally, we show that recombinant TRPM3, as well as the endogenous TRPM3 in insuloma cells, is rapidly and reversibly inhibited by activation of phospholipase C–coupled muscarinic acetylcholine receptors. Our results reveal basic cellular mechanisms whereby membrane receptors can regulate TRPM3 activity.

INTRODUCTION

TRPM3 is a calcium-permeable nonselective cation channel belonging to the melastatin subfamily of TRP channels (Grimm et al., 2003; Oberwinkler and Philipp, 2014). TRPM3 is highly expressed in a subset of sensory neurons, and its activation by the neurosteroid pregnenolone sulfate (PregS) or by noxious heat evokes pain in mice (Vriens et al., 2011). Importantly, TRPM3-deficient mice failed to develop inflammatory heat hyperalgesia, suggesting that the channel may be sensitized in the context of inflamed tissue (Vriens et al., 2011). TRPM3 is also highly expressed in pancreatic β cells, where its activation by PregS enhances glucose-induced insulin release (Wagner et al., 2008, 2010), as well as in variety of other tissues, where its function remains to be fully elucidated (Oberwinkler and Philipp, 2014). To better understand the (patho)physiological roles of TRPM3, detailed knowledge of its cellular regulation is essential. Currently very little is known about possible intracellular modulators of TRPM3. Biochemical evidence suggested Ca^{2+}-dependent binding of calmodulin and S100A1 to the N terminus of TRPM3, but the functional impact of this interaction on TRPM3 function is unknown (Holakovska et al., 2012).

Signal transduction events modulating TRP channels frequently involve direct interaction between the channels and regulatory molecules, including plasma membrane phosphoinositides such as phosphatidylinositol 4,5-bisphosphate (PI(4,5)P_2; Hilgemann et al., 2001; Runnels et al., 2001; Nilius et al., 2008; Suh and Hille, 2008; Rohacs, 2014). Because plasma membrane levels of phosphoinositides are under the control of phospholipases, phosphatidylinositol kinases and phosphatidylinositol phosphatases, this represents an important general mechanism to modulate TRP channels function downstream of metabotropic receptor stimulation (Julius and Basbaum, 2001; Nilius et al., 2008). Here, we provide evidence for a direct regulation of TRPM3 by PIPs. Our results link TRPM3 to various cellular signaling pathways downstream of receptor stimulation, which may shape sensory processes, insulin release and other cellular events involving TRPM3.

The Rockefeller University Press $30.00
J. Gen. Physiol. Vol. 146 No. 1 51–63
www.jgp.org/cgi/doi/10.1085/jgp.201411339

51

MATERIALS AND METHODS

Cell culture and heterologous expression

HEK293T cells stably overexpressing the mouse TRPM3α2 variant (HEK-M3 cells) or human TRPM8 (HEK-M8 cells) were generated and cultured as described before (Mahieu et al., 2010; Vriens et al., 2011; Drews et al., 2014). Ins1 cells were cultured in RPMI Medium 1640 supplemented with 10% FBS (both from Life Technologies Ltd.), 1 mM Na-pyruvate, 10 mM HEPES, 1% Penicillin/Streptomycin, and 50 µM β-Mercaptoethanol (all supplements from Sigma-Aldrich).

HEK-M3 cells were transiently transfected by various constructs using Mirus TransIT-293 (Mirus Corporation). For transfection, the following constructs were used: Ci-VSP and Ci-VSP C363S (Murata et al., 2005; provided by Y. Okamura, Osaka University, Osaka, Japan); mRFP-FKBP-5-ptase-dom, mRFP-FKBP-only, PM-FRB-mRFP, or PM-FRB-CFP and PLCδ$_1$PH-GFP (Varnai et al., 2006; T. Balla, National Institutes of Health, Bethesda, MD); the M1 muscarinic receptor; and Dr-VSP (Hossain et al., 2008; D. Oliver, University of Marburg, Marburg, Germany).

Electrophysiology

Whole-cell, cell-attached, and inside-out patch-clamp recordings were performed using an EPC-10 amplifier and Patchmaster software (HEKA Elektronik; Lambrecht/Pfalz Germany) or an Axopatch 200B amplifier and PClamp software (Molecular Devices). Data were sampled at 5–20 kHz and digitally filtered off-line at 1–5 kHz. Unless mentioned otherwise, the holding potential was 0 mV and cells were ramped every 2 s from −150 to +150 mV over the course of 200 ms. In Ins1 cells and indicated experiments on HEK293 cells, a ramp from −115 to +85 mV was applied from a −15 mV holding potential. When using Dr-VSP, ramps were limited to +45 mV, to avoid activation of the phosphatase during the ramp. Pipettes with final resistances of 2–5 MΩ were fabricated and filled with either extracellular or intracellular solution. The extracellular solution of HEK-M3 cells generally contained 150 mM NaCl, 1 mM MgCl$_2$, and 10 mM HEPES buffered to pH 7.4 (NaOH). Because free Mg^{2+} in the cytosolic solution inhibits TRPM3 activity (Oberwinkler et al., 2005), we kept the calculated free Mg^{2+} in the different intracellular solutions constant at 0.7 mM, unless mentioned otherwise. To determine the free Mg^{2+} concentrations, we used the CaBuf program (available as Supplemental material http://perswww.kuleuven.be/~u0032053/CaBuf.zip), which takes into account the K$_d$ values for Mg^{2+} of the various Mg^{2+}-chelating compounds, including ATP, EGTA, and aspartate. The standard intracellular solution contained 100 mM aspartic acid, 45 mM CsCl, 1.144 mM MgCl$_2$, 10 mM HEPES, and 10 mM EGTA (pH 7.2 using CsOH). In the solutions containing 2 mM ATP or 2 mM AMPPCP, we further included 2 mM Na$_2$ATP (or Na$_2$AMPPCP) and increased the total MgCl$_2$ to 2.99 mM. The Mg^{2+}-free intracellular solution contained 100 mM aspartic acid, 45 mM CsCl, 10 mM HEPES, and 10 mM EDTA (pH 7.2 with CsOH). When measuring Dr-VSP and M1 muscarinic receptor transfected HEK-M3 cells, the following solutions were applied: extracellular solution: 145 mM NaCl, 10 mM CsCl, 3 mM KCl, 2 mM CaCl$_2$, 2 mM MgCl$_2$, 10 mM HEPES, and 10 mM glucose pH 7.2 (by NaOH); intracellular solution: 80 mM aspartate, 50 mM CsCl, 10 mM BAPTA (or 5 mM EGTA, as indicated), 10 mM HEPES, 4 mM Na$_2$ATP, 3 mM MgCl$_2$, and 120 mM CsOH (pH 7.2). In some experiments, Li$_4$AMPPNP was substituted for Na$_2$ATP and only 1 mM MgCl$_2$ was added. The extracellular solution for Ins1 cells consisted of 145 mM NaCl, 10 mM CsCl, 3 mM KCl, 2 mM CaCl$_2$, 2 mM MgCl$_2$, 10 mM HEPES, 3 mM glucose, and 7 mM D-mannitol, pH 7.2 (by NaOH), and the intracellular solution was the same as in case of Dr-VSP–transfected HEK-M3 cells. In inside-out and cell-attached measurements, 100 µM PregS was added to the patch pipette to activate TRPM3. All measurements were performed at room temperature. Liquid junction potentials were corrected for off-line.

Fluorescence microscopy

Fura-2–based ratiometric intracellular Ca^{2+} measurements were performed as described previously (Wagner et al., 2008; Vriens et al., 2011). In brief, cells were loaded with 2 µM Fura-2 AM dye in culture medium for 30–45 min at 37°C, and intracellular Ca^{2+} concentration was monitored as the ratio of fluorescence intensities upon illumination at 340 and 380 nm using an MT-10 illumination system and Olympus xcellence pro software (Olympus). Experiments on HEK-M3 cells were performed in extracellular solution containing 150 mM NaCl, 1 mM MgCl$_2$, 2 mM CaCl$_2$, and 10 mM HEPES buffered to pH 7.4 (NaOH).

Translocation of PLCδ$_1$PH-GFP from plasma membrane to cytosol was monitored on an Axio Observer.Z1 microscope (Carl Zeiss) equipped with a 100× oil objective having numerical aperture of 1.45 and a Hamamatsu Orca-R2 camera. CFP-, GFP-, and RFP-fluorescence were measured sequentially using 405-, 488-, and 561-nm excitation lasers and tailor-made band-pass filters, and time series of images at 6-s intervals were recorded. At the start of the experiment, the focus was set such that PLCδ$_1$PH-GFP was observed as a clear border surrounding the cell image. Constant focus was ensured using the Definite Focus module (Carl Zeiss). Translocation of PLCδ$_1$PH-GFP was quantified as the ratio between the GFP fluorescence in a region of interest covering the center of the cell (excluding the outermost 20%) and the total fluorescence of the cell, and normalized to the ratio before stimulation with rapamycin.

Chemicals

The TRPM3 agonist PregS and TRPM8 agonist menthol were purchased from Sigma-Aldrich. ATP was purchased from Roche. The nonhydrolyzable ATP analogue adenosine-5-[(β,γ)-methyleno]triphosphate (AMPPCP) was obtained from Jena Bioscience and adenosine-5-[(β,γ)-imido]triphosphate (AMPPNP) was purchased from Sigma-Aldrich. Water-soluble diC8 PIPs and diC16 PI(4,5)P$_2$ were purchased from Echelon, IP$_3$ was obtained from Sigma-Aldrich, and brain-derived natural PI(4,5)P$_2$ was obtained from Avanti. Stock solutions of PIPs were reconstituted in H$_2$O and stored at −80°C, and they were intensively sonicated before use. Estimated mole fractions in the inner leaflet of the membrane for diC8- PI(4,5)P$_2$ and diC8- PI(4)P were calculated based on the polynomial functions provided in Collins and Gordon (2013), which provide a relationship between PIP concentrations in solution and their distribution in artificial liposomes. To scavenge PIPs, poly-L-lysine (PLL) and neomycin were used (both from Sigma-Aldrich). The phosphatidylinositol-3 kinase (PI-3K) inhibitors wortmannin and LY294,002, as well as rapamycin were from LC Laboratories. The mAChR receptors were activated by oxotremorine-M (N,N,N-trimethyl-4-(2-oxo-1-pyrolidinyl)-2-butyn-1-ammonium iodide; Oxo-M) from BioTrend Chemicals.

Statistical analysis

Electrophysiological data were analyzed using WinASCD software (Guy Droogmans). Origin 8.6 (OriginLab Corporation) and SPSS 9.0 (SPSS Inc.) were used for statistical analysis and data display. For statistical comparison, Student's unpaired or paired t tests, or one-way ANOVA with Dunnett or Bonferroni post-hoc test were applied, as appropriate. All data are presented as mean ± SEM.

Online supplemental material

A zip file with the application and information to run the CaBuf program is available at http://www.jgp.org/cgi/content/full/jgp.201411339/DC1.

RESULTS

TRPM3 is regulated by the cellular environment

To assess the influence of the intracellular environment on TRPM3 activity, we performed cell-free inside-out patch clamp measurements in HEK-M3 cells. TRPM3 channels were stimulated by 100 µM PregS applied to the extracellular side via the pipette solution. In the cell attached configuration, before excision of the inside-out patch, we measured an outwardly rectifying current, as described earlier (Wagner et al., 2008; Vriens et al., 2014; Fig. 1, A and B). Outward current amplitudes increased dramatically upon excision of the inside-out patch. The peak TRPM3 current measured at +120 mV showed a large variation in amplitude (from several tens to several hundred of pAs), most probably depending on the actual expression of the channel in the excised membrane patches. Similar experiments performed on nontransfected HEK293T cells ($n = 10$) or on HEK-M3 when omitting PregS from the pipette solution ($n = 10$) yielded only small and linear currents that did not increase in amplitude upon patch excision, as described earlier (Vriens et al., 2014), showing that the pattern described in Fig. 1 represents TRPM3 activity. The current increase upon excision was followed by rapid current run-down (Fig. 1 A). The sudden increase of the TRPM3 current amplitude upon excision could be explained by a sudden loss of inhibitory cytoplasmic factors, whereas the subsequent run-down may results from loss cytoplasmic factors that are required for sustaining channel activity. We therefore aimed at finding which regulatory factors influence TRPM3 activity.

PI(4,5)P$_2$ and ATP restore TRPM3 activity

PI(4,5)P$_2$ is a minor constituent of cellular membranes, representing <1% of the total membrane phospholipids (Czech, 2000). Nevertheless, PI(4,5)P$_2$ plays an important role in the regulation of ion channels, including inhibitory and activating effects on several TRP channels. Intracellular ATP is also known to modulate the activity of several TRP channels, in part by influencing the available PI(4,5)P$_2$ level in the plasma membrane (Rohacs and Nilius, 2007; Voets and Nilius, 2007; Nilius et al., 2008; Rohacs, 2014). Thus, we tested the effect of PI(4,5)P$_2$ and ATP on TRPM3 currents in excised membrane patches. Application of diC8 PI(4,5)P$_2$ (a water-soluble PI(4,5)P$_2$ analogue) to the cytosolic side of inside-out patches resulted in a dose-dependent and reversible restoration of TRPM3 currents (Fig. 1, C and D). At 10 and 50 µM diC8 PI(4,5)P$_2$, corresponding to estimated mole fractions of PI(4,5)P$_2$ in the inner leaflet of the membrane patch of 0.003 and 0.01 (Collins and Gordon, 2013), recovery amounted to $30 \pm 5\%$ and $69 \pm 9\%$, respectively (Fig. 1, C, D, and I). Application of 2 mM ATP to the cytosolic side of the excised membrane patches, at a constant free Mg^{2+} concentration of 0.7 mM, also restored the TRPM3 activity with a very characteristic biphasic time course (Fig. 1, E and F). The TRPM3 current recovered only partially during application of ATP, but showed a more complete and long lasting recovery after wash-out of the ATP ($115 \pm 11\%$; Fig. 1, E, F, and I). The biphasic current restoration by ATP could be repeated with similar efficiency within the same patch (Fig. 1 E). These results can be explained by assuming that Mg-ATP has both an activating and an inhibitory effect on TRPM3 and that the inhibitory effect is rapidly reversible, whereas the activating effect is more long lasting. This interpretation is also supported by the finding that the typical sudden current increase was not observed when patch excision was performed in a solution containing ATP (Fig. 1 G). A slower but more pronounced current recovery was also observed when using the natural, brain-derived form of PI(4,5)P$_2$ (10 µM), which contains longer fatty acid chains making it poorly water soluble (Fig. 1, H and I). However, the outcome of these experiments was quite variable, due to precipitation and formation of lipid droplets in our aqueous buffers, and the fact that recommended organic solvents to solubilize the natural form of PI(4,5)P$_2$ often caused disruption of the inside-out patches. Application of inositol 1,4,5-triphosphate (I(1,4,5)P$_3$), the polar head group of PI(4,5)P$_2$, was fully ineffective at concentrations up to 100 µM ($n = 3$; <5% recovery; not depicted).

ATP-induced recovery of TRPM3 activity involves resynthesis of PI-phosphates

The robust and long-lasting current restoration after ATP application suggested the involvement of ATP-using enzymes in the restoration of TRPM3 current. Considering that most ATP-consuming enzymes require Mg-ATP as a substrate, we tested the effect of cytosolic ATP in Mg^{2+}-free solution. Importantly, under this condition ATP completely failed to restore TRPM3 activity (Fig. 2 A; $n = 10$). Moreover, the nonhydrolyzable ATP analogue AMPPCP ($n = 4$) was fully ineffective in restoring TRPM3 activity. These data provide strong evidence that the restoration of TRPM3 activity depends on membrane-delimited ATP hydrolysis and on ATP-metabolizing enzymes that remain preserved in inside-out membrane patches. In this respect, phosphatidylinositol-kinases (PI-Ks) such as phosphatidylinositol-4-kinases (PI-4Ks) are known to remain active in cell-free patches, regenerating PI(4,5)P$_2$, which is known to regulate the activity of various channels and transporters (Balla, 2001; Hilgemann et al., 2001; Nilius et al., 2008). Earlier work has also demonstrated that in inside-out patch clamp recordings ATP can restore PI(4,5)P$_2$ levels in the membrane by stimulating the activity of PI-Ks, which explains the long lasting stimulating effect of ATP on the activity of TRPV6 (Zakharian et al., 2011), TRPM8 (Yudin et al., 2011) or TRPM4 (Nilius et al., 2006). To assess whether
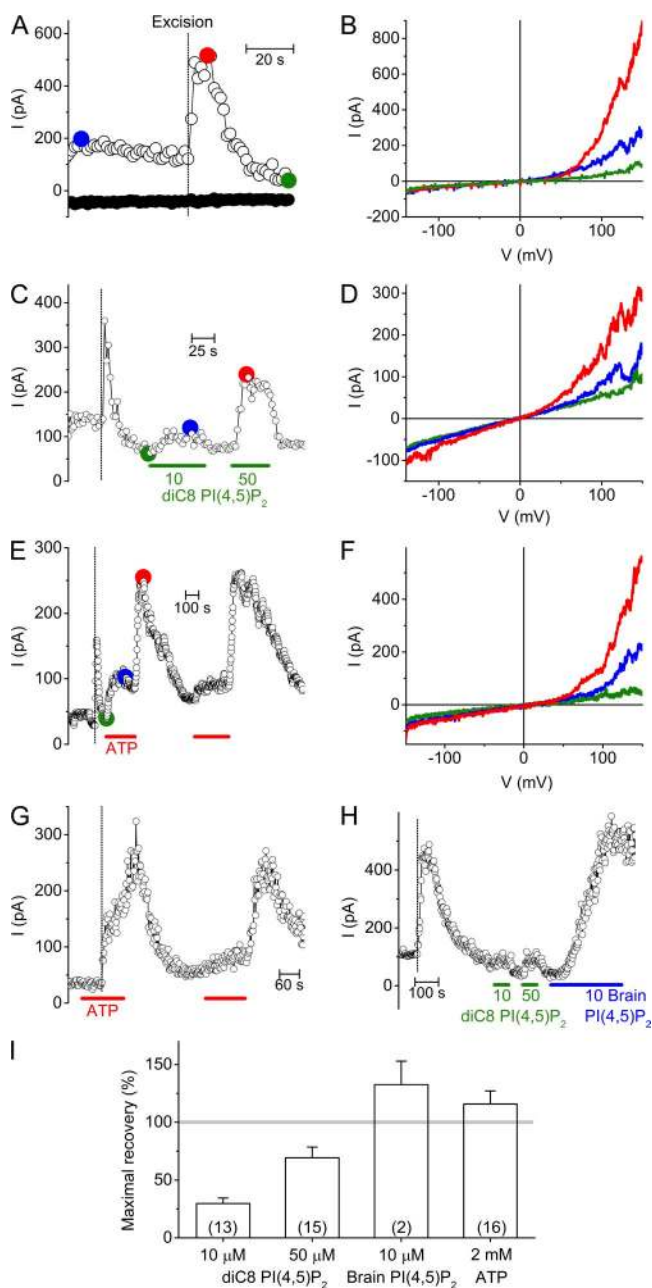
Figure 1. Decay and recovery of TRPM3 activity in inside-out membrane patches. (A) Time course of TRPM3 currents at -120 and $+120$ mV in cell-attached mode and, after patch-excision, in cell-free inside-out patch from a HEK-M3 cell. TRPM3 was activated by inclusion of 100 µM PregS in the extracellular (pipette) solution. The vertical dotted line in this and subsequent panels indicates the time point of patch excision. Membrane patches were always excised into intracellular solution. (B) I-V traces at different time points as indicated in A. (C) Representative time course showing the effect of diC8 $PI(4,5)P_2$ on TRPM3 currents measured in inside-out configuration. (D) I-V traces at different time points as indicated in C. (E) Representative time course showing the effect of 2 mM ATP on TRPM3 currents measured in inside-out configuration. (F) I-V traces at different time points as indicated in E. (G) Representative time course showing the effect of 2 mM ATP on TRPM3 current upon excision. (H) Representative time course comparing the effects of diC8 and brain derived natural $PI(4,5)P_2$ applied to the cytoplasmic side of an inside-out

the ATP-induced restoration of TRPM3 activity was due to resynthesis of $PI(4,5)P_2$ and/or related PI-phosphates, we first tested the effect of poly-L-lysine (PLL) and neomycin, two positively charged molecules that are able to scavenge the negative charges of PI-phosphates, thereby preventing their interaction with membrane proteins (Gamper and Shapiro, 2007; Suh and Hille, 2007; Nilius et al., 2008; Leitner et al., 2011). We found that, after current restoration by ATP pretreatment, application of PLL (50 µg/ml) or neomycin (5 mM) to the cytosolic side of the excised membrane patches rapidly inhibited the TRPM3 current (Fig. 2, C–E). Next, we tested whether pharmacological inhibition of enzymes involved in resynthesis of PI-phosphates were able to prevent the restoration of TRPM3 by ATP. First, preapplication of Wortmannin to inside-out patches, at a concentration (50 µM) where it inhibits various kinases (including PI-3K and PI-4K), largely prevented the ATP-evoked TRPM3 current recovery (Fig. 2, F and H). A similar, robust but incomplete inhibition was obtained with LY294,002, another PI-K inhibitor (Fig. 2, G and H), at a concentration (300 µM) where it blocks both PI-3K and PI-4K (Knight et al., 2006). Collectively, these data indicate that the restoration of TRPM3 activity by cytosolic ATP is (at least partly) a result of resynthesis of membrane PIPs through the activity of PI-Ks.

Partial inhibition of TRPM3 by PIP 5-phosphatase

Plasma membrane levels of $PI(4,5)P_2$ (and of the less abundant $PI(3,4,5)P_3$) can be rapidly and specifically reduced by the activity of 5-phosphatases. To test the effect of depletion of the endogenous $PI(4,5)P_2$ and $PI(3,4,5)P_3$ in intact cells, we combined intracellular calcium imaging with the use of a recombinant mRFP-FKBP12 linked PIP 5-phosphatase domain (mRFP-FKBP-5-ptase-dom) that can be directly targeted to the plasma membrane by a short rapamycin application in the presence of an FRB-coupled membrane linker (PM-FRB-mRFP or PM-FRB-CFP; Varnai et al., 2006). Application of 1 µM rapamycin led to a rapid decrease in the membrane $PI(4,5)P_2$ level, as indicated by the rapid translocation from the plasma membrane to the cytosol by the $PLC\delta_1$ PH domain fused to GFP ($PLC\delta_1$PH-GFP) in HEK-M3 cells coexpressing PM-FRB-CFP and mRFP-FKBP-5-ptase-dom, but not in cells expressing the same constructs without having the 5-phosphatase domain (PM-FRB-CFP and mRFP-FKBP-only; Fig. 3, A and B). In spite of the rapid $PI(4,5)P_2$ degradation, PregS-induced Ca^{2+} transients in HEK-M3 cells cotransfected with mRFP-FKBP-5-ptase-dom, PM-FRB-mRFP and $PLC\delta_1$PH-GFP

excised membrane patch. (I) Maximal current recovery evoked by $PI(4,5)P_2$ and ATP. Currents were normalized to the peak current upon excision. Numbers of individual membrane patches are indicated in parentheses.
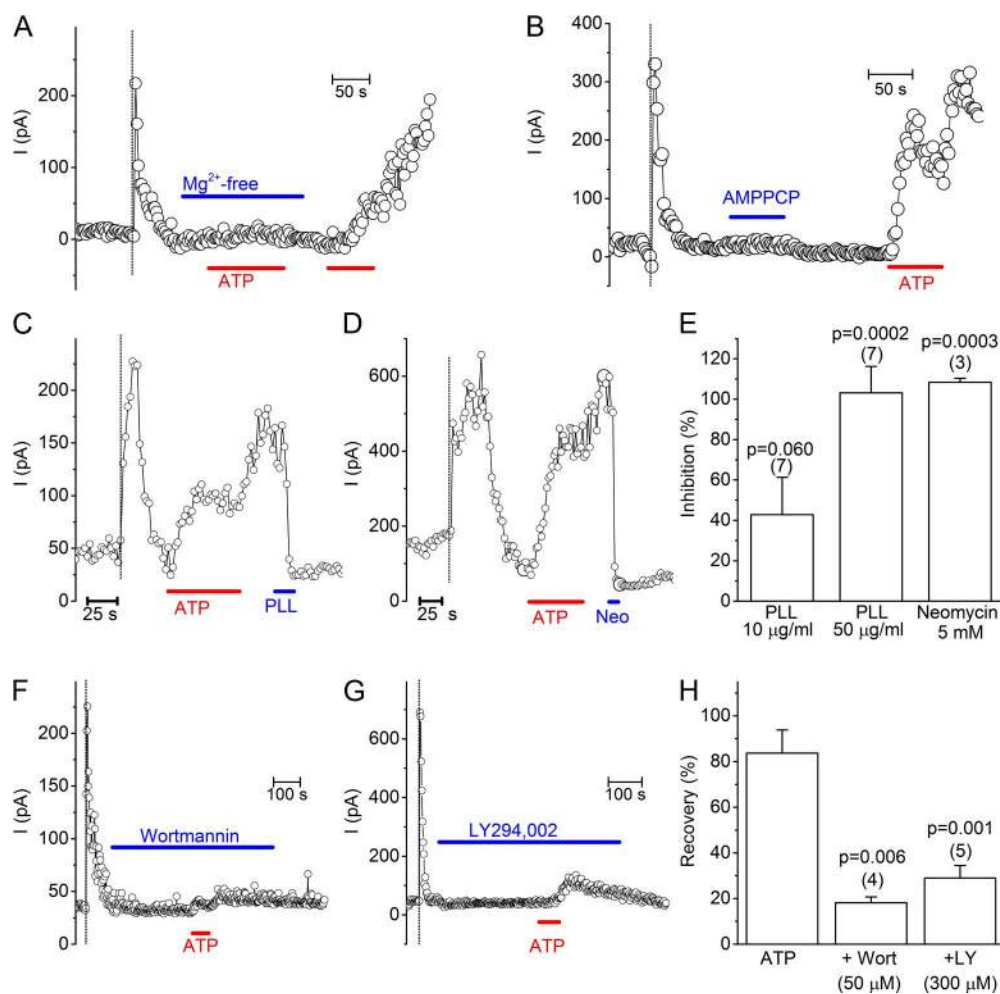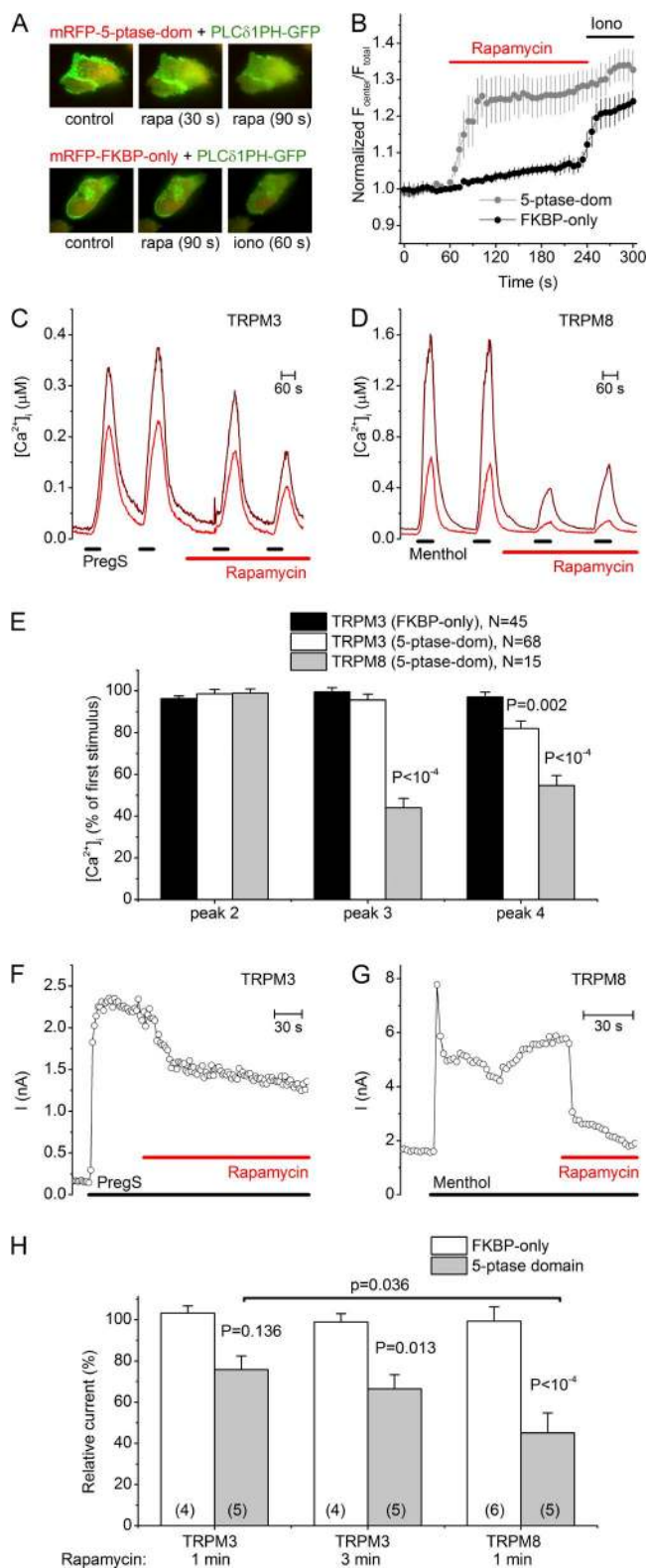
Figure 2. ATP-induced recovery of TRPM3 requires PI-kinase activity. (A) Representative time course showing the lack of current recovery (<5%) upon ATP application in Mg^{2+}-free solution. (B) Representative time course showing the lack of current recovery (<5%) upon application of AMPPCP (2 mM). (C and D) Representative time courses showing the rapid inhibition of TRPM3 activity by the PIP scavengers PLL (50 µg/ml) and Neomycin (5 mM) applied to the cytoplasmic side of inside-out membrane patches. (E) Statistical analysis of current inhibition at +120 mV by the various PIP scavenging agents. Values are given as percentage of the ATP-induced current recovery just before the application of the compound. P-values were determined by using one sample Student's t test. (F and G) Representative time courses showing the impaired ATP-induced recovery of TRPM3 activity in the presence of the PI-kinase inhibitors wortmannin and LY294,002. (H) Comparison of the ATP-induced current recovery in the absence and presence of PI-kinase inhibitors. P-values were obtained by one-way ANOVA, with Bonferroni post-hoc test to compare with the inhibitor-free condition.

were reduced by only ∼20% after prolonged rapamycin treatment (Fig. 3, C and E). In comparison, menthol-induced Ca^{2+} transients in cells expressing TRPM8 along with the rapamycin-inducible system were reduced more rapidly and profoundly after application of 1 µM rapamycin, in line with previous work (Varnai et al., 2006; $56 \pm 5\%$ reduction after a 2-min application of rapamycin; Fig. 3, D and E). Overall, these results indicate that depletion of $PI(4,5)P_2$ by 5-phosphatases can cause a significant but partial inhibition of TRPM3 activity in intact cells. The incompleteness of the inhibitory effect observed may indicate that the $PI(4,5)P_2$ reduction in intact cells, despite the significant translocation of $PLC\delta_1PH$-GFP, is insufficient to cause full inhibition of TRPM3 activity. In whole-cell current measurements using an ATP-containing intracellular solution, the rapamycin-inducible system was slightly more efficient but the TRPM3 current inhibition was again only partial, and

the effect was slower and less pronounced than for TRPM8 tested under identical conditions ($24 \pm 7\%$ and $55 \pm 10\%$ current inhibition after 1 min of rapamycin for TRPM3 and TRPM8, respectively; Fig. 3, F–H).

To further investigate the role of $PIP(4,5)P_2$ depletion in the control of TRPM3 activity, we used whole-cell current measurements in HEK-M3 cells expressing Ci-VSP, a voltage-gated PIP 5-phosphatase from *Ciona intestinalis* (Murata et al., 2005). The 5-phosphatase activity of this enzyme is coupled to a voltage-sensing domain similar to the voltage sensor domain (S1-S4) of voltage-gated ion channels, such that depolarization activates the phosphatase and results in strong hydrolysis of the phosphate group at the 5 position of $PI(4,5)P_2$ and $PI(3,4,5)$ P_3 (Murata and Okamura, 2007; Iwasaki et al., 2008; Halaszovich et al., 2009). In whole-cell patch-clamp measurements, we regulated the activity of Ci-VSP by varying the holding potential between -70 and $+90$ mV and

tested TRPM3 activity during short (100-ms) ramps from -150 to $+150$ mV. The pipette solution contained 2 mM ATP to ensure substrate for PI-Ks to restore $PI(4,5)P_2$ during the hyperpolarizing intervals. The depolarization partially inhibited the PregS-induced TRPM3 currents in cells expressing wild-type Ci-VSP ($37 \pm 5\%$ inhibition), but not in cells expressing the Ci-VSP C363S mutation, which results in a loss-of-function phenotype of the phosphatase catalytic domain (Fig. 4, A–D and G). This indicates that the phosphate group at the 5 position of $PI(4,5)P_2$ and/or $PI(3,4,5)P_3$ is required to sustain maximal TRPM3 activity. Because Ci-VSP already shows a marked activation at 0 mV, it is possible that the applied voltage ramp caused substantial $PI(4,5)P_2$ depletion, even at -70 mV holding potential. Therefore, we performed similar experiments using the voltage-activated phosphatase of the *Danio rerio* (Dr-VSP), whose activation curve is shifted to more positive voltages, with significant activity requiring depolarization >50 mV (Hossain et al., 2008). In these experiments, we limited the voltage ramp to +45 mV and activated Dr-VSP by a 1-s depolarizing prepulse (+100 mV) before each ramp in the test period. Under this condition, TRPM3 was more effectively inhibited ($67 \pm 3\%$ inhibition) than with Ci-VSP, but nevertheless $\sim$30% of the current remained (Fig. 4, E–F and H). It is important to mention that the end-products of the 5-phosphatase reaction, especially the most common metabolite $PI(4)P$, may also influence TRP channel activity, as was described for TRPV1 and TRPM4 (Nilius et al., 2006; Lukacs et al., 2007, 2013). Importantly, in the presence of intracellular ATP, the currents rapidly recovered after activation of Ci-VSP and Dr-VSP. However, when ATP in the intracellular solution was substituted by the

Figure 3. Effect of a translocatable PI 5-phosphatase on TRPM3 activity in HEK-M3 cells. (A) Fluorescence images showing the translocation of the $PI(4,5)P_2$ sensor PLCδ$_1$ PH-GFP (green) in HEK-M3 cells. These cells further expressed an FRB coupled plasma membrane linker (PM-FRB-CFP; not depicted) together with either mRFP-FKBP-5-ptase-dom (top; red) or mRFP-FKBP-only (bottom; red), before and after application of 1 µM rapamycin or 10 µM ionomycin. (B) Mean time course ($n = 5$ for each condition) of the normalized ratio between the GFP fluorescence in the cell center and the entire cell, as a measure of PLCδ$_1$ PH-GFP translocation from plasma membrane to cytosol. (C) Two representative intracellular Ca^{2+} traces upon repetitive stimulation with PregS (10 µM) in HEK-M3 cells overexpressing PM-FRB-mRFP and mRFP-FKBP-5-ptase-dom, before and after rapamycin-induced $PI(4,5)P_2$ breakdown. (D) Same as C, but in HEK cells expressing human TRPM8 instead of TRPM3, repetitively stimulated with menthol (50 µM). (E) Amplitude of the second-fourth calcium transients, normalized to the first calcium transient, for the indicated conditions. P values were obtained by unpaired Student's *t* test, comparing with the mRFP-FKBP-only condition. (F) Representative time course of PregS-induced (40 µM) current inhibition upon rapamycin-induced $PI(4,5)P_2$ breakdown in HEK-M3 cells. (G) Same as F, but in HEK cells expressing human TRPM8 instead of TRPM3, stimulated with menthol (50 µM). (H) Analysis of the effect of rapamycin-induced $PI(4,5)P_2$ breakdown in HEK cells expressing either TRPM3 or TRPM8. PregS- and menthol-induced currents measured in the presence of rapamycin were normalized to the current measured just before the application of rapamycin. P values were obtained by one-way ANOVA and Bonferroni post-hoc test, comparing with the mRFP-FKBP-only condition or as indicated.
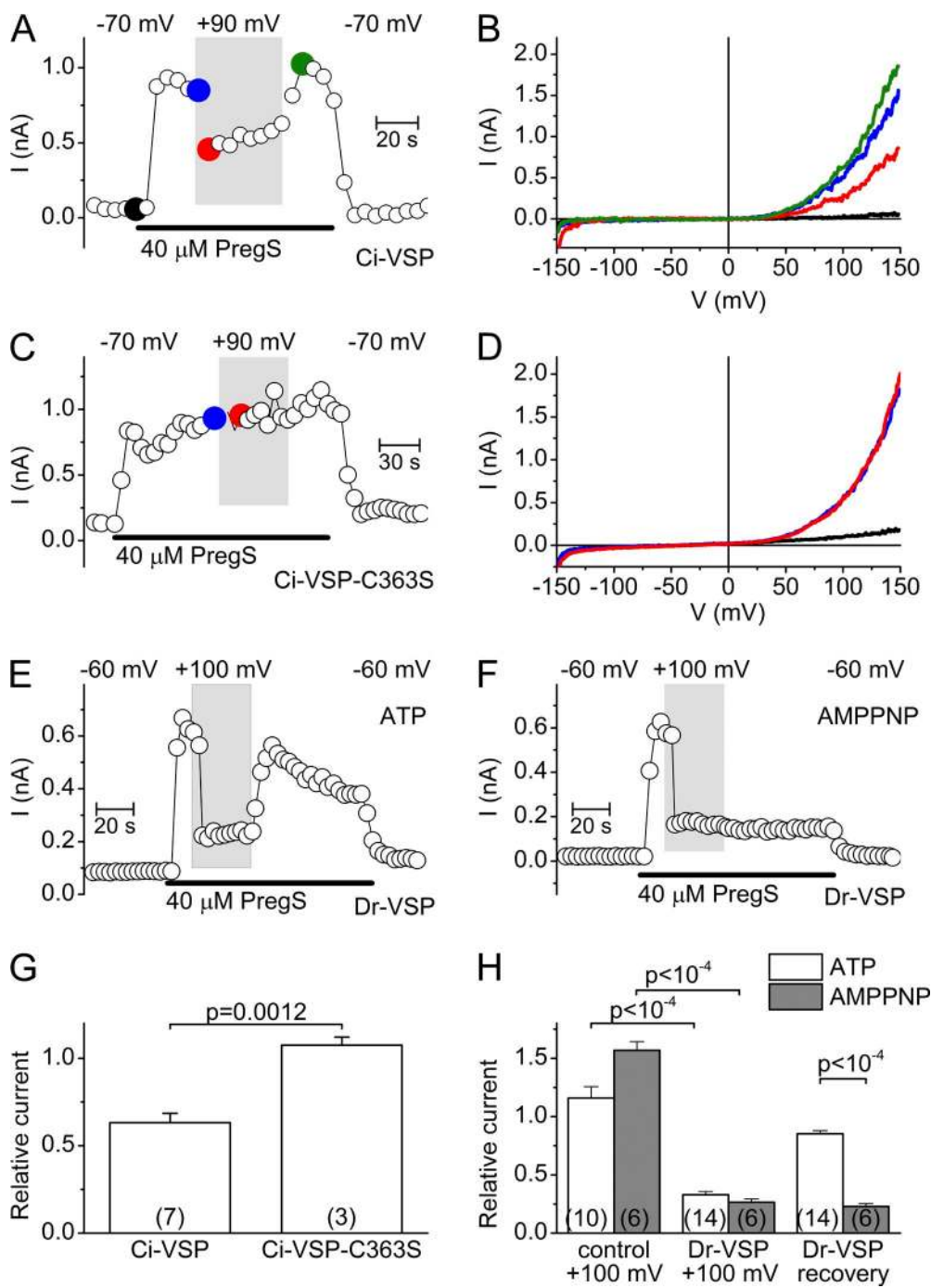
Figure 4. Effect of voltage-sensitive 5-phosphatases on TRPM3 whole-cell currents. (A) Representative time course of whole-cell currents measured at +120 mV in a cell coexpressing TRPM3 and Ci-VSP, illustrating the effect of changing holding potential from -70 to +90 mV (white and gray background, respectively). (B) I-V traces at different time points indicated in *A*. (C and D) Same as in A and B, except for a cell transfected with inactive mutant Ci-VSP-C363S. (E) Representative time course of whole-cell currents measured at +40 mV in a cell coexpressing TRPM3 and Dr-VSP, illustrating the effect of changing holding potential from -60 to +100 mV (white and gray background, respectively) using an intracellular solution containing 4 mM ATP. (F) Same as E, but using an intracellular solution containing 4 mM AMPPNP. (G) Comparison of relative currents measured at +120 mV and with a depolarizing holding potential (+90 mV) in cells expressing Ci-VSP and Ci-VSP-C363S. Currents were normalized to the currents measured at a -70-mV holding potential. P-values were obtained by unpaired Student's *t* test. (H) Comparison of relative currents measured at +40 mV and with a depolarizing holding potential (+100 mV) in cells expressing TRPM3 without (control) or with Dr-VSP, for the conditions described in E and F. Current were normalized to the currents measured at a -60-mV holding potential. P-values were obtained by one-way ANOVA, with Bonferroni post-hoc.

nonhydrolyzable analogue AMPPNP, recovery was abolished, indicating that ATP hydrolysis is essential for the current restoration after 5-phosphatase activation (Fig. 4, F and H). Collectively, the results using various 5-phosphatases indicate that depletion of plasma membrane $PI(4,5)P_2$ (and possible $PI(3,4,5)P_3$) levels cause a significant but incomplete inhibition of TRPM3 activity, and indicate that, in intact cells, the effects of $PI(4,5)P_2$ depletion are counteracted by ATP-dependent resynthesis.

Recovery of TRPM3 activity by different PIPs

The finding that depletion of endogenous $PI(4,5)P_2$, using a variety of techniques, leads to only a partial inhibition of TRPM3 activity prompted us to test the effect of other PIPs, which, although normally present at lower levels than $PI(4,5)P_2$, may support TRPM3 activity. Therefore, we compared the effect of the water-soluble (diC8) forms of $PI(4)P$, $PI(3,4)P_2$, $PI(3,5)P_2$, $PI(4,5)P_2$ and $PI(3,4,5)P_3$ at a fixed concentration (50 µM) on the
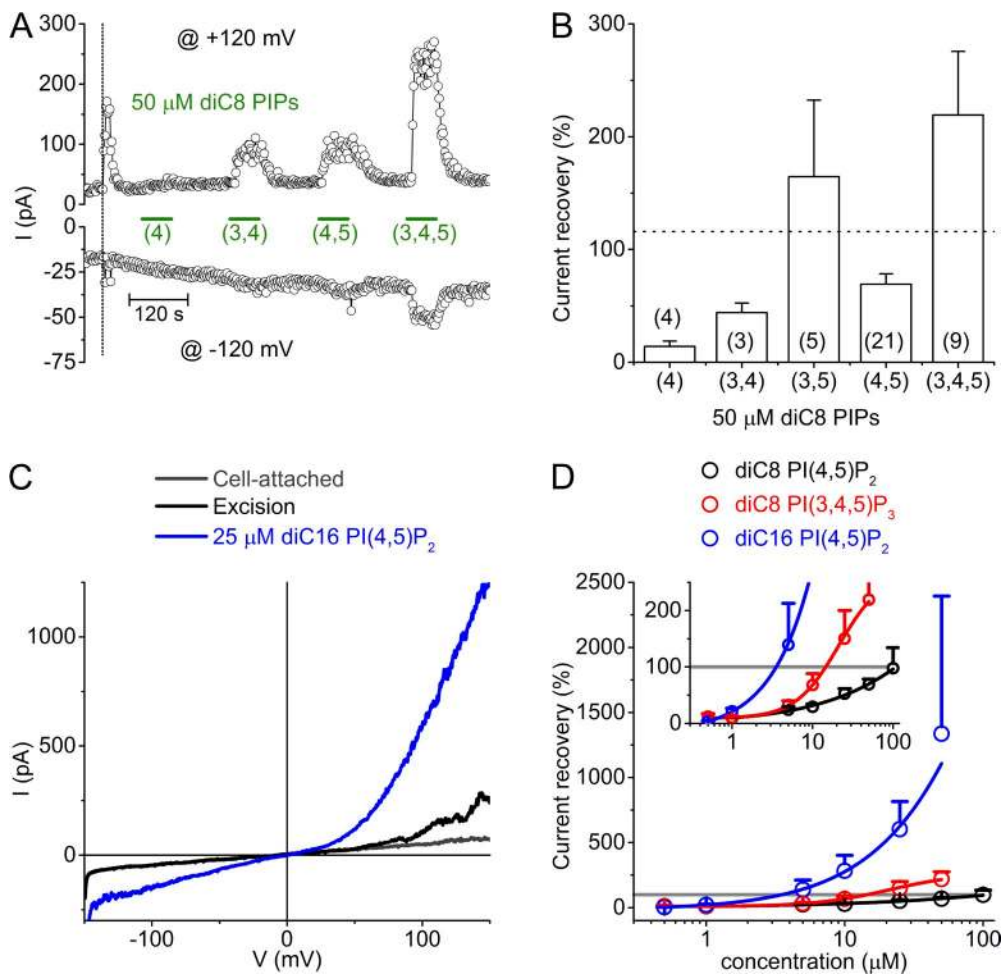
Figure 5. Comparison of TRPM3 recovery by different PIPs. (A) Representative time course showing variable recovery of TRPM3 activity in an inside-out patch upon application of the indicated diC8 PIPs at a concentration of 50 µM. (B) Statistical analysis of the current recovery at +120 mV by 50 µM of the indicated diC8 PIPs. The dotted line indicates the mean recovery obtained with 2 mM ATP. Numbers of individual membrane patches are in parentheses. (C) Representative I-V curves showing the current response to 25 µM diC16 $PI(4,5)P_2$. (D) Dose dependence of the effect of diC8 $PI(4,5)P_2$, diC8 $PI(3,4,5)P_3$ and diC16 $PI(4,5)P_2$. Currents were normalized to the peak current upon excision (indicated by the gray line). n = 2–21/data point. Solid lines represent a logistic function fitted to the data. Since saturation could not be obtained at the highest testable concentrations, reliable EC_{50} values could not be obtained. The inset shows a magnification of the lower part of the dose–response graph, allowing estimation of the concentrations required to obtain 100% current recovery.

recovery of TRPM3 activity in inside-out patches. This revealed that PI(4)P, at an estimated mole fraction in the inner leaflet of the membrane of 0.02 (Collins and Gordon, 2013), had only a minimal effect (14 ± 5% recovery) and that $PI(3,4)P_2$ (44 ± 9%) was almost equally effective as $PI(4,5)P_2$ (69 ± 9%), whereas $PI(3,5)P_2$ (165 ± 68%) and especially $PI(3,4,5)P_3$ (219 ± 56%) were more effective than $PI(4,5)P_2$ (Fig. 5, A and B). In particular, $PI(3,4,5)P_3$ already had a marked effect at 5 µM, and at 50 µM it evoked a current amplitude that was on average twofold larger than the current amplitude upon excision, or of the level of current recovery induced by $PI(4,5)P_2$ or 2 mM ATP (Fig. 5). These results indicate that TRPM3 is rather nonselective toward PIPs. Nevertheless, it is questionable whether the more effective $PI(3,4,5)P_3$ may contribute to the sustained level of TRPM3 activity upon depletion of $PI(4,5)P_2$, as its concentration in the plasma membrane, even in stimulated cells, does not exceed a few percent of that of $PI(4,5)P_2$. Moreover, $PI(3,4,5)P_3$ is hardly detectable in nonstimulated cells (Czech, 2000; Knight et al., 2006).

Whereas the exogenous diC8 $PI(4,5)P_2$ resulted in a partial restoration of TRPM3 activity, the limited results using brain-derived $PI(4,5)P_2$ raised the possibility that channel activity can be more efficiently restored by $PI(4,5)P_2$ forms with longer acyl chains. This is also supported by our findings that ATP was superior to diC8 $PI(4,5)P_2$ in restoring TRPM3 activity. Application of diC16 $PI(4,5)P_2$, a $PI(4,5)P_2$ analogue with longer acyl chains, indeed resulted in a very robust potentiation of TRPM3 currents (Fig. 5, C and D), far beyond peak current levels upon patch excision, and this potentiating effect did not clearly saturate at the maximal concentrations that could be obtained in solution. To compare the relative potency of the different PIP isoforms, we estimated the concentration at which they were able to restore current levels to 100% of the TRPM3 current upon excision, based on concentration-response relationships. This analysis indicates that diC16 $PI(4,5)P_2$ can restore the current level upon excision at a concentration as low as 3.5 µM, compared with 14.5 µM for diC8 $PI(3,4,5)P_3$ and ∼100 µM for diC8 $PI(4,5)P_2$ (Fig. 5 D).
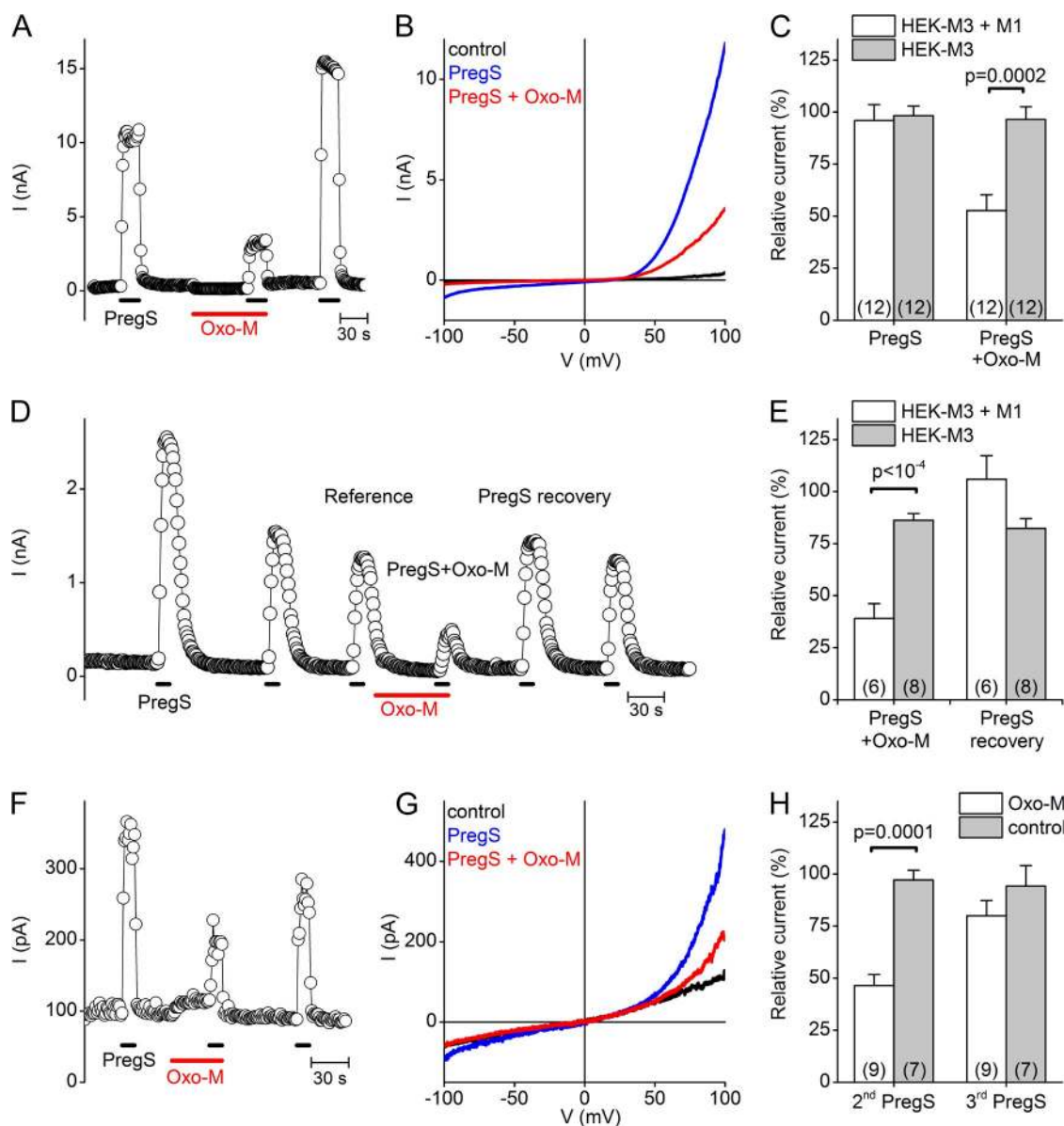
Figure 6. Reversible inhibition of whole-cell TRPM3 currents by muscarinic receptor stimulation. (A) Representative time course of whole-cell currents in a HEK-M3 cell heterologously expressing the M1 mAChR, illustrating the reversible effect of M1 stimulation by 20 µM Oxo-M in the presence of 10 mM BAPTA in the intracellular solution. (B) Representative I-V traces for the experiment in *A*. (C) Relative amplitude of the current response to the second PregS application, normalized to the mean of the first and third responses, comparing the effect of vehicle or Oxo-M in HEK-M3 cells with or without expression of the M1 mAChR. (D) Same as *A,* but in the presence of 5 mM EGTA instead of BAPTA in the intracellular solution. (E) Relative amplitude of the current response to PregS in the presence of Oxo-M and after the Oxo-M wash out, normalized to the PregS response before the Oxo-M application, showing the effect of Oxo-M on HEK-M3 cells with or without expressing the M1 mAChR. (F and G) Same as in A and B, except in an Ins1 cell, which endogenously expressed TRPM3 and mAChR. (H) Comparison of the relative current amplitude of the second and third (recovery) response to the initial PregS application, in cells stimulated with Oxo-M or vehicle. P-values in C, E, and H were obtained by unpaired Student's *t* tests.

Partial inhibition of TRPM3 by PLC-coupled receptor activation

Finally, we asked whether activation of PLC-coupled receptors can influence TRPM3 activity. To test this, we overexpressed the M1 muscarinic acetylcholine receptor (mAChR) in HEK-M3 cells and investigated the effect of the mAChR agonist Oxo-M on TRPM3

activity. In these experiments, 10 mM BAPTA was included in the pipette solution to fully suppress increases in cytosolic Ca^{2+}. Similar to the voltage-activated phosphatases, activation of the M1 mAChR resulted in a significant but partial decrease of PregS-evoked TRPM3 currents ($47 \pm 8\%$ decrease in TRPM3 current, compared with $4 \pm 6\%$ reduction in cell that did

not express the M1 receptor; Fig. 6, A–C). The addition of 10 mM BAPTA to the intracellular solution rapidly binds all Ca^{2+} flowing into the cytosol, and thereby strongly suppresses all Ca^{2+}-dependent downstream signaling events. However, these strong buffering conditions may also impair PLC-mediated PI(4,5)P_2 degradation, as was shown for M1 mAChR regulation of KCNQ channels (Horowitz et al., 2005). Therefore, we repeated these experiments using 5 mM EGTA, resulting in a less stringent and slower buffering of intracellular Ca^{2+}. In this case, we experienced a marked but incomplete rundown of TRPM3 currents upon repeated PregS application, consistent with our previous findings (Vriens et al., 2011, 2014). To minimize the interference of channel run-down, we first applied three pulses of PregS, coapplied Oxo-M during the fourth application, and normalized this last response to the response to the third PregS application (Fig. 6, D–E). Under these conditions, M1 receptor activation evoked a current inhibition that was slightly more pronounced in comparison to the 10 mM BAPTA condition (61 ± 7% decrease in the presence vs. 13 ± 3% in the absence of M1), but still incomplete.

Because activation of recombinant M1 mAChR effectively inhibited TRPM3 responses, we investigated the role of endogenous PLC-coupled signal transduction in the control of native TRPM3. To this end, we investigated the PregS-evoked TRPM3 responses in the rat insulinoma-derived Ins1 cell line, which endogenously expresses functional TRPM3 (Wagner et al., 2008). In Ins1 cells, activating the endogenous mAChRs with Oxo-M (again in the presence of 10 mM BAPTA) also resulted in a marked inhibition of the PregS-induced TRPM3 currents (Fig. 6, F–H). This inhibition was reversible in the presence of ATP in the intracellular solution. Collectively, these results indicate that both overexpressed and endogenous TRPM3 can be dynamically inhibited by receptor-mediated activation of PLC, independently of intracellular Ca^{2+} signals.

DISCUSSION

In recent years, TRPM3 has emerged as a nociceptor channel highly expressed in a subset of sensory neurons, playing a key role as a primary sensor of acute heat and specific chemical stimuli. Importantly, there is evidence that TRPM3 is involved in the development of inflammatory hyperalgesia and that pharmacological inhibition of TRPM3 may alleviate neuropathic pain, suggesting that TRPM3 activity is modulated by signaling processes that are active in the context of inflammation or nerve injury (Vriens et al., 2011; Straub et al., 2013; Chen et al., 2014). Moreover, TRPM3 was found to be functionally expressed in pancreatic β cells, where its activity may be coupled to insulin secretion (Wagner et al., 2008). However, little was known about the cellular mechanisms and signaling pathways that regulate TRPM3 activity. In this study, we provide evidence for a dynamic regulation of TRPM3 by plasma membrane PIPs. In particular, we demonstrate that ATP applied to the cytosolic side exhibits a strong stimulatory effect on TRPM3 activity, which requires the activity of PI-kinases resulting in the (re)synthesis of PIPs. Moreover, we found that PI(4,5)P_2 and other PIPs have a direct stimulatory effect on TRPM3 activity in cell-free inside-out patches. Finally, we show that various maneuvers that lead to an acute reduction of the plasma membrane levels of PIPs, especially the most abundant one (PI[4,5]P_2), including application of nonspecific PIP scavengers, activation of 5-phosphatases, and activation of PLC-coupled receptors, lead to a reduction of TRPM3 activity.

In our patch clamp recordings, we observed that TRPM3 activity transiently increased, in comparison to the current level in the cell-attached mode, upon inside-out patch excision, and subsequently decayed to a level comparable or below the current level measured in cell attached configuration. Our data show that peak current levels can be restored by application of Mg-ATP to the cytosolic side of the patch, which we attribute to restoration of plasma membrane levels of PI(4,5)P_2 and other PIPs. This conclusion is based on the findings that current restoration (a) required hydrolysable ATP in the presence of Mg^{2+}, (b) was reversed by agents that scavenge PIPs, (c) was inhibited by pharmacological block of PI-K activity, and (d) was mimicked by direct application of PIPs to the cytosolic side of the patch. A similar ATP-driven restoration of PI(4,5)P_2 levels in the plasma membrane has been reported to restore the activity of various other TRP channels, including TRPM8, TRPM4, TRPA1, or TRPV6 (Rohács et al., 2005; Nilius et al., 2006, 2008; Karashima et al., 2008; Zakharian et al., 2011). The initial rapid increase in current amplitude upon patch excision most likely reflects the sudden loss of one or more cytosolic factors that negatively regulate TRPM3 activity, and we hypothesize that Mg-ATP itself may be such an inhibitory factor. In line with this, we consistently observed (a) that current restoration by Mg-ATP exhibited a clear "off" response, suggesting an inhibitory effect of Mg-ATP that is rapidly reversed upon wash-out, whereas the Mg-ATP–induced restoration of PIP levels is more long-lasting, and (2) that the presence of Mg-ATP abolished the characteristic rapid current increase upon patch excision.

The use of inside-out patches allowed us to directly compare the ability of various PIPs in restoring TRPM3 activity. Applying the water soluble diC8 forms, we found that PI(3,4,5)P_3 was by far the most effective, able to provoke current levels that exceeded the peak current upon excision by more than twofold. PI(3,5)P_2 was also superior to PI(4,5)P_2, PI(3,4)P_2 displayed almost the same efficacy as PI(4,5)P_2, and PI(4)P was practically ineffective. The PIP selectivity profile (PI(3,4,5)P_3 > PI(3,5)P_2 > PI(4,5)P_2 PI(3,4)P_2 PI(4)P) of TRPM3 is

clearly distinct from that of related TRPM channels TRPM8 and TRPM4, which exhibit a clear selectivity for $PI(4,5)P_2$ versus other PIPs (Rohács et al., 2005; Nilius et al., 2006). This difference in PIP selectivity may be reflected in a different sensitivity to cellular signals. For instance, to our knowledge, TRPM3 shows the highest selectivity toward $PI(3,4,5)P_3$ among all TRP channels. This raises the possibility that increases in cellular $PI(3,4,5)P_3$ levels, which can be evoked by receptor-mediated activation of PI-3K, may enhance TRPM3 activity in stimulated cells. Although cellular $PI(3,4,5)P_3$ levels, even following stimulation of PI-3K, do not exceed a few percent of the $PI(4,5)P_2$ levels (Czech, 2000), localized rises in $PI(3,4,5)P_3$ may have an impact on TRPM3 activity. Clearly, further research is required to establish whether activation of PI-3K, e.g., after stimulation of neurotrophin receptors, can enhance TRPM3 activity in sensory neurons or other cell types.

To selectively assess the consequences of $PI(4,5)P_2$ depletion in whole cells, we used various 5-phosphatases that can be rapidly switched on and off, either by changing the membrane potential (Ci-VSP and Dr-VSP; Murata et al., 2005; Murata and Okamura, 2007) or by rapamycin-induced targeting to the plasma membrane (FKBP-5-phase; Varnai et al., 2006). In whole-cell patch clamp measurements, voltage-dependent activation of the VSPs resulted in an immediate but incomplete inhibition of TRPM3 current, which was rapidly reversed in the presence of intracellular ATP but not when ATP was substituted by a nonhydrolysable analogue. Depleting the endogenous $PI(4,5)P_2$ by using the rapamycin-induced targeting of a 5-phosphatase to the plasma membrane also resulted in a significant decrease of TRPM3 responses. However, under similar conditions, inhibition of TRPM8 activity by 5-phosphatase activity was much faster and more pronounced. The fact that maximal activation of 5-phosphatases consistently resulted in only a partial inhibition of TRPM3 indicates that TRPM3 has a relatively high affinity for membrane-associated $PI(4,5)P_2$, such that the low level of $PI(4,5)P_2$ that remains after 5-phosphatase activation is sufficient to sustain significant channel activity. Whereas results obtained using the diC8 form of $PI(4,5)P_2$ seemed to argue against such a high affinity, our findings that the long acyl chain-containing diC16 $PI(4,5)P_2$ and natural brain-derived $PI(4,5)P_2$ can restore current levels at low micromolar concentrations are consistent with such a relatively high affinity. For instance, diC16 $PI(4,5)P_2$ restored 100% of the TRPM3 current upon excision at concentrations as low as 5 µM, and at higher concentrations we observed currents that were several-fold larger than the current upon excision. Considering the relative promiscuity of TRPM3 toward various PIPs, we cannot exclude the possibility that PIPs other than $PI(4,5)P_2$, such as $PI(3,4)P_2$, may also contribute to sustaining normal TRPM3 activity.

In addition to 5-phosphatase activity, $PI(4,5)P_2$ levels can rapidly drop as a result of the activity of PLC enzymes. Different isoforms of PLC are activated by various processes, in particular activation of Go/Gq-coupled GPCRs, tyrosine kinase receptors and rises in intracellular Ca^{2+} concentration (Rebecchi and Pentyala, 2000). Rapid depletion of $PI(4,5)P_2$ by PLC activation has been shown to quickly influence the activity of TRPM4 (Nilius et al., 2006), TRPM8 (Rohács et al., 2005; Liu and Qin, 2005), or TRPV1 (Chuang et al., 2001) activity. Similarly, our present results show that activation of the PLC-coupled M1 muscarinic acetylcholine receptor caused a marked block of TRPM3 upon heterologous expression in HEK cells. Moreover, we demonstrate that the endogenous TRPM3 current in Ins1 cells is reversibly inhibited by activation of endogenous mAChR, independent of the release of Ca^{2+} from intracellular stores, providing a first example of TRPM3 regulation downstream of the activation of a metabotropic membrane receptor. Although our results are in line with a mechanism whereby PLC-coupled receptors act on TRPM3 via $PI(4,5)P_2$ depletion, it cannot be excluded that intracellular Ca^{2+} release and/or activation of protein kinase C (PKC) downstream of PLC activation modulate TRPM3 activity as well.

In the general context of $PI(4,5)P_2$ regulation of ion channels, our results suggest that TRPM3 has a low specificity and relatively high affinity toward $PI(4,5)P_2$. However, a simple comparison of dose–response curves for the effect of $PI(4,5)P_2$ on channel activity, when applied to the cytosolic side of a membrane patch, may not be the best way to compare $PI(4,5)P_2$ affinities in a physiologically meaningful way. Indeed, as we show here, such apparent affinities can depend strongly on the lengths of the acyl chains of $PI(4,5)P_2$, which vary between studies. Moreover, patch excision can lead to loss of cellular factors that affect channel regulation or PIP metabolism. Therefore, sensitivity to depletion of endogenous $PI(4,5)P_2$ in intact cells or whole-cell recordings is arguably a better way to compare $PI(4,5)P_2$ affinity in a physiologically relevant manner (Kruse et al., 2012). In the case of the related TRP channels TRPM6 and TRPM8, depletion of cellular $PI(4,5)P_2$ using either the rapamycin-inducible 5-phosphatase system, Ci-VSP or PLC-coupled receptor activation causes an almost complete inhibition (>90%) of the whole-cell currents (Rohács et al., 2005; Varnai et al., 2006; Xie et al., 2011; Yudin et al., 2011). The partial inhibition of TRPM3 activity, typically not >50%, which we observed with these same $PI(4,5)P_2$-depleting maneuvers suggests that TRPM3 has a higher affinity toward membrane $PI(4,5)P_2$ than these other TRPM channels. In addition, our results indicate that PIPs other than $PI(4,5)P_2$ can restore TRPM3 activity, which may also contribute to the sustained currents after strong $PI(4,5)P_2$ depletion. The same $PI(4,5)P_2$-depleting tools have also been extensively used to

compare phosphoinositide regulation of various potassium channels, revealing a broad spectrum of apparent $PI(4,5)P_2$ sensitivities. For instance, $K_V7.2/7.3$ (KCNQ2/3) channels are rapidly and almost completely (>90%) inhibited by activation of Dr-VSP or PLC-coupled receptors, whereas $K_{ir}2.1$ is only partially (∼45%) blocked by Dr-VSPs and not significantly affected by mAChR receptor activation, and several other K_V channels (e.g., members of the K_V1, K_V2, K_V3, K_V4 and K_V11 subfamilies) are not detectably affected by $PI(4,5)P_2$ depletion (Rohács et al., 1999; Sakata et al., 2011; Kruse et al., 2012). As such, TRPM3 appears to be in the middle of the spectrum of $PI(4,5)P_2$ sensitivities, allowing for significant functional regulation upon receptor-mediated activation of PLC.

In conclusion, we provide evidence for a tight regulation of TRPM3 by plasma membrane levels of $PI(4,5)P_2$ and related PIPs. These represent potent cellular mechanisms whereby membrane receptors may impact on TRPM3 function, for instance in sensory neurons under inflammatory conditions.

REFERENCES

Balla, T. 2001. Pharmacology of phosphoinositides, regulators of multiple cellular functions. *Curr. Pharm. Des.* 7:475–507. http://dx.doi.org/10.2174/1381612013397906

Chen, L., W. Chen, X. Qian, Y. Fang, and N. Zhu. 2014. Liquiritigenin alleviates mechanical and cold hyperalgesia in a rat neuropathic pain model. *Sci Rep.* 4:5676.

Chuang, H.H., E.D. Prescott, H. Kong, S. Shields, S.E. Jordt, A.I. Basbaum, M.V. Chao, and D. Julius. 2001. Bradykinin and nerve growth factor release the capsaicin receptor from PtdIns(4,5)P2-mediated inhibition. *Nature.* 411:957–962. http://dx.doi.org/10.1038/35082088

Collins, M.D., and S.E. Gordon. 2013. Short-chain phosphoinositide partitioning into plasma membrane models. *Biophys. J.* 105:2485–2494. http://dx.doi.org/10.1016/j.bpj.2013.09.035

Czech, M.P. 2000. PIP2 and PIP3: complex roles at the cell surface. *Cell.* 100:603–606. http://dx.doi.org/10.1016/S0092-8674(00)80696-0

Drews, A., F. Mohr, O. Rizun, T.F. Wagner, S. Dembla, S. Rudolph, S. Lambert, M. Konrad, S.E. Philipp, M. Behrendt, et al. 2014. Structural requirements of steroidal agonists of transient receptor potential melastatin 3 (TRPM3) cation channels. *Br. J. Pharmacol.* 171:1019–1032. http://dx.doi.org/10.1111/bph.12521

Gamper, N., and M.S. Shapiro. 2007. Regulation of ion transport proteins by membrane phosphoinositides. *Nat. Rev. Neurosci.* 8:921–934. http://dx.doi.org/10.1038/nrn2257

Grimm, C., R. Kraft, S. Sauerbruch, G. Schultz, and C. Harteneck. 2003. Molecular and functional characterization of the melastatin-related cation channel TRPM3. *J. Biol. Chem.* 278:21493–21501. http://dx.doi.org/10.1074/jbc.M300945200

Halaszovich, C.R., D.N. Schreiber, and D. Oliver. 2009. Ci-VSP is a depolarization-activated phosphatidylinositol-4,5-bisphosphate and phosphatidylinositol-3,4,5-trisphosphate 5'-phosphatase. *J. Biol. Chem.* 284:2106–2113. http://dx.doi.org/10.1074/jbc.M803543200

Hilgemann, D.W., S. Feng, and C. Nasuhoglu. 2001. The complex and intriguing lives of PIP2 with ion channels and transporters. *Sci. STKE.* 2001:re19.

Holakovska, B., L. Grycova, M. Jirku, M. Sulc, L. Bumba, and J. Teisinger. 2012. Calmodulin and S100A1 protein interact with N terminus of TRPM3 channel. *J. Biol. Chem.* 287:16645–16655. http://dx.doi.org/10.1074/jbc.M112.350686

Horowitz, L.F., W. Hirdes, B.C. Suh, D.W. Hilgemann, K. Mackie, and B. Hille. 2005. Phospholipase C in living cells: activation, inhibition, Ca2+ requirement, and regulation of M current. *J. Gen. Physiol.* 126:243–262. http://dx.doi.org/10.1085/jgp.200509309

Hossain, M.I., H. Iwasaki, Y. Okochi, M. Chahine, S. Higashijima, K. Nagayama, and Y. Okamura. 2008. Enzyme domain affects the movement of the voltage sensor in ascidian and zebrafish voltage-sensing phosphatases. *J. Biol. Chem.* 283:18248–18259. http://dx.doi.org/10.1074/jbc.M706184200

Iwasaki, H., Y. Murata, Y. Kim, M.I. Hossain, C.A. Worby, J.E. Dixon, T. McCormack, T. Sasaki, and Y. Okamura. 2008. A voltage-sensing phosphatase, Ci-VSP, which shares sequence identity with PTEN, dephosphorylates phosphatidylinositol 4,5-bisphosphate. *Proc. Natl. Acad. Sci. USA.* 105:7970–7975. http://dx.doi.org/10.1073/pnas.0803936105

Julius, D., and A.I. Basbaum. 2001. Molecular mechanisms of nociception. *Nature.* 413:203–210. http://dx.doi.org/10.1038/35093019

Karashima, Y., J. Prenen, V. Meseguer, G. Owsianik, T. Voets, and B. Nilius. 2008. Modulation of the transient receptor potential channel TRPA1 by phosphatidylinositol 4,5-biphosphate manipulators. *Pflugers Arch.* 457:77–89. http://dx.doi.org/10.1007/s00424-008-0493-6

Knight, Z.A., B. Gonzalez, M.E. Feldman, E.R. Zunder, D.D. Goldenberg, O. Williams, R. Loewith, D. Stokoe, A. Balla, B. Toth, et al. 2006. A pharmacological map of the PI3-K family defines a role for p110alpha in insulin signaling. *Cell.* 125:733–747. http://dx.doi.org/10.1016/j.cell.2006.03.035

Kruse, M., G.R. Hammond, and B. Hille. 2012. Regulation of voltage-gated potassium channels by PI(4,5)P2. *J. Gen. Physiol.* 140:189–205. http://dx.doi.org/10.1085/jgp.201210806

Leitner, M.G., C.R. Halaszovich, and D. Oliver. 2011. Aminoglycosides inhibit KCNQ4 channels in cochlear outer hair cells via depletion of phosphatidylinositol(4,5)bisphosphate. *Mol. Pharmacol.* 79:51–60. http://dx.doi.org/10.1124/mol.110.068130

Liu, B., and F. Qin. 2005. Functional control of cold- and menthol-sensitive TRPM8 ion channels by phosphatidylinositol 4,5-bisphosphate. *J. Neurosci.* 25:1674–1681. http://dx.doi.org/10.1523/JNEUROSCI.3632-04.2005

Lukacs, V., B. Thyagarajan, P. Varnai, A. Balla, T. Balla, and T. Rohacs. 2007. Dual regulation of TRPV1 by phosphoinositides. *J. Neurosci.* 27:7070–7080. http://dx.doi.org/10.1523/JNEUROSCI.1866-07.2007

Lukacs, V., Y. Yudin, G.R. Hammond, E. Sharma, K. Fukami, and T. Rohacs. 2013. Distinctive changes in plasma membrane phosphoinositides underlie differential regulation of TRPV1 in

nociceptive neurons. *J. Neurosci.* 33:11451–11463. http://dx.doi.org/10.1523/JNEUROSCI.5637-12.2013

Mahieu, F., A. Janssens, M. Gees, K. Talavera, B. Nilius, and T. Voets. 2010. Modulation of the cold-activated cation channel TRPM8 by surface charge screening. *J. Physiol.* 588:315–324. http://dx.doi.org/10.1113/jphysiol.2009.183582

Murata, Y., and Y. Okamura. 2007. Depolarization activates the phosphoinositide phosphatase Ci-VSP, as detected in Xenopus oocytes coexpressing sensors of PIP2. *J. Physiol.* 583:875–889. http://dx.doi.org/10.1113/jphysiol.2007.134775

Murata, Y., H. Iwasaki, M. Sasaki, K. Inaba, and Y. Okamura. 2005. Phosphoinositide phosphatase activity coupled to an intrinsic voltage sensor. *Nature.* 435:1239–1243. http://dx.doi.org/10.1038/nature03650

Nilius, B., F. Mahieu, J. Prenen, A. Janssens, G. Owsianik, R. Vennekens, and T. Voets. 2006. The Ca2+-activated cation channel TRPM4 is regulated by phosphatidylinositol 4,5-biphosphate. *EMBO J.* 25:467–478. http://dx.doi.org/10.1038/sj.emboj.7600963

Nilius, B., G. Owsianik, and T. Voets. 2008. Transient receptor potential channels meet phosphoinositides. *EMBO J.* 27:2809–2816. http://dx.doi.org/10.1038/emboj.2008.217

Oberwinkler, J., and S.E. Philipp. 2014. Trpm3. *Handbook Exp. Pharmacol.* 222:427–459.

Oberwinkler, J., A. Lis, K.M. Giehl, V. Flockerzi, and S.E. Philipp. 2005. Alternative splicing switches the divalent cation selectivity of TRPM3 channels. *J. Biol. Chem.* 280:22540–22548. http://dx.doi.org/10.1074/jbc.M503092200

Rebecchi, M.J., and S.N. Pentyala. 2000. Structure, function, and control of phosphoinositide-specific phospholipase C. *Physiol. Rev.* 80:1291–1335.

Rohacs, T. 2014. Phosphoinositide regulation of TRP channels. *Handbook Exp. Pharmacol.* 223:1143–1176.

Rohacs, T., and B. Nilius. 2007. Regulation of transient receptor potential (TRP) channels by phosphoinositides. *Pflugers Arch.* 455:157–168. http://dx.doi.org/10.1007/s00424-007-0275-6

Rohács, T., J. Chen, G.D. Prestwich, and D.E. Logothetis. 1999. Distinct specificities of inwardly rectifying K(+) channels for phosphoinositides. *J. Biol. Chem.* 274:36065–36072. http://dx.doi.org/10.1074/jbc.274.51.36065

Rohács, T., C.M. Lopes, I. Michailidis, and D.E. Logothetis. 2005. PI(4,5)P2 regulates the activation and desensitization of TRPM8 channels through the TRP domain. *Nat. Neurosci.* 8:626–634. http://dx.doi.org/10.1038/nn1451

Runnels, L.W., L. Yue, and D.E. Clapham. 2001. TRP-PLIK, a bifunctional protein with kinase and ion channel activities. *Science.* 291:1043–1047. http://dx.doi.org/10.1126/science.1058519

Sakata, S., M.I. Hossain, and Y. Okamura. 2011. Coupling of the phosphatase activity of Ci-VSP to its voltage sensor activity over the entire range of voltage sensitivity. *J. Physiol.* 589:2687–2705. http://dx.doi.org/10.1113/jphysiol.2011.208165

Straub, I., U. Krügel, F. Mohr, J. Teichert, O. Rizun, M. Konrad, J. Oberwinkler, and M. Schaefer. 2013. Flavanones that selectively inhibit TRPM3 attenuate thermal nociception in vivo. *Mol. Pharmacol.* 84:736–750. http://dx.doi.org/10.1124/mol.113.086843

Suh, B.C., and B. Hille. 2007. Electrostatic interaction of internal Mg2+ with membrane PIP2 Seen with KCNQ K+ channels. *J. Gen. Physiol.* 130:241–256. http://dx.doi.org/10.1085/jgp.200709821

Suh, B.C., and B. Hille. 2008. PIP2 is a necessary cofactor for ion channel function: how and why? *Annu. Rev. Biophys.* 37:175–195. http://dx.doi.org/10.1146/annurev.biophys.37.032807.125859

Varnai, P., B. Thyagarajan, T. Rohacs, and T. Balla. 2006. Rapidly inducible changes in phosphatidylinositol 4,5-bisphosphate levels influence multiple regulatory functions of the lipid in intact living cells. *J. Cell Biol.* 175:377–382. http://dx.doi.org/10.1083/jcb.200607116

Voets, T., and B. Nilius. 2007. Modulation of TRPs by PIPs. *J. Physiol.* 582:939–944. http://dx.doi.org/10.1113/jphysiol.2007.132522

Vriens, J., G. Owsianik, T. Hofmann, S.E. Philipp, J. Stab, X. Chen, M. Benoit, F. Xue, A. Janssens, S. Kerselaers, et al. 2011. TRPM3 is a nociceptor channel involved in the detection of noxious heat. *Neuron.* 70:482–494. http://dx.doi.org/10.1016/j.neuron.2011.02.051

Vriens, J., K. Held, A. Janssens, B.I. Tóth, S. Kerselaers, B. Nilius, R. Vennekens, and T. Voets. 2014. Opening of an alternative ion permeation pathway in a nociceptor TRP channel. *Nat. Chem. Biol.* 10:188–195. http://dx.doi.org/10.1038/nchembio.1428

Wagner, T.F., S. Loch, S. Lambert, I. Straub, S. Mannebach, I. Mathar, M. Düfer, A. Lis, V. Flockerzi, S.E. Philipp, and J. Oberwinkler. 2008. Transient receptor potential M3 channels are ionotropic steroid receptors in pancreatic beta cells. *Nat. Cell Biol.* 10:1421–1430. http://dx.doi.org/10.1038/ncb1801

Wagner, T.F., A. Drews, S. Loch, F. Mohr, S.E. Philipp, S. Lambert, and J. Oberwinkler. 2010. TRPM3 channels provide a regulated influx pathway for zinc in pancreatic beta cells. *Pflugers Arch.* 460:755–765. http://dx.doi.org/10.1007/s00424-010-0838-9

Xie, J., B. Sun, J. Du, W. Yang, H.C. Chen, J.D. Overton, L.W. Runnels, and L. Yue. 2011. Phosphatidylinositol 4,5-bisphosphate (PIP(2)) controls magnesium gatekeeper TRPM6 activity. *Sci. Rep.* 1:146. http://dx.doi.org/10.1038/srep00146

Yudin, Y., V. Lukacs, C. Cao, and T. Rohacs. 2011. Decrease in phosphatidylinositol 4,5-bisphosphate levels mediates desensitization of the cold sensor TRPM8 channels. *J. Physiol.* 589:6007–6027. http://dx.doi.org/10.1113/jphysiol.2011.220228

Zakharian, E., C. Cao, and T. Rohacs. 2011. Intracellular ATP supports TRPV6 activity via lipid kinases and the generation of PtdIns(4,5)P$_2$. *FASEB J.* 25:3915–3928. http://dx.doi.org/10.1096/fj.11-184630